Photoconductivity, low-temperature conductivity, and magnetoresistance studies on the layered semiconductor GaTe

D. N. Bose[1] and Sarbari Pal[2]
[1]*Advanced Technology Center, Indian Institute of Technology, Kharagpur 721 302 India*
[2]*Department of Physics, Indian Institute of Technology, Kharagpur 721 302 India*
(Received 20 November 2000; published 31 May 2001)

Single crystals of *p*-GaTe were grown by the Bridgman technique and characterized through x-ray diffraction, energy-dispersive x-ray analysis, x-ray photoemission spectroscopy, and transmission electron microscopy studies. The photoconductivity spectral response for in-plane conduction showed a peak at 747 nm (1.66 eV). Photoconductivity gain was determined in two orthogonal directions from which the majority carrier (hole) lifetimes were found to be 3.43×10^{-7} and 2.03×10^{-6} s, respectively, parallel and perpendicular to the layer planes. Studies of the temperature dependence of conductivity in the directions along and perpendicular to the layer planes were carried out between 10 and 80 K. Along the layer planes the conductance $G_{\parallel}$ varied as $\ln T$ between 12 and 20 K, characteristic of weak localization, while between 20 and 50 K the conductivity $\sigma_{\parallel}$ varied as $T^{1/2}$. In the perpendicular direction the conductance $G_{\perp}$ varied as $\exp(T/T_0)^{1/3}$ between 9 and 20 K and the conductivity $\sigma_{\perp}$ varied as $\exp(T/T_0)^{1/4}$ between 20 and 50 K, characteristic of hopping conduction in two and three dimensions, respectively. Negative transverse magnetoresistance was observed at 10 K for conduction in both directions for magnetic fields $H<0.4$ T, the increase in conductance being found to be proportional to H^2. Band conduction with positive magnetoresistance was observed for both current directions at $T>70$ K. The *I-V* characteristics at 10 K showed quantized behavior due to electron tunneling across potential barriers caused by stacking faults between layer planes.

DOI: 10.1103/PhysRevB.63.235321 PACS number(s): 72.80.Jc, 72.20.Fr, 72.40.+w, 73.20.Fz

I. INTRODUCTION

Layered semiconductors have always been of interest due to their anisotropic properties, resulting from strong covalent bonding within the layer planes and weak van der Waals type bonding between them.[1] Recent interest is due to their possible applications in van der Waals epitaxy.[2] It has also been found that during epitaxial growth of II-VI compounds on III-V substrates III-VI compounds such as GaSe and GaTe are formed as intermediate layers.[3] GaTe crystallizes in the monoclinic system (space group C_2^2). According to the Mooser-Pearson criterion it is a III-VI semiconductor having one cation-cation (*M-M*) bond and forming *X-M-M-X* chains. GaTe has a more complex structure than GaS and GaSe with two different types of Ga-Ga bond. Different polytypes β, δ, and ε, with space groups D_{6h}^4, D_{3h}^1, and D_{3v}^5 have also been reported.

Fischer and Brebner[4] studied the resistivity and Hall effect in GaTe single crystals between 80 and 1000 K. All their samples, regardless of the low-temperature properties, exhibited intrinsic behavior above 600–700 K. In this range the in-plane resistivity $\rho_{\parallel}=\rho_{\perp}$, the resistivity normal to the layer plane, while between 100 and 300 K the crystals were *p* type with anisotropy $\rho_{\perp}/\rho_{\parallel}=30-70$. The effect of cold working was found to increase both resistivity and Hall coefficient, which was attributed to the creation of new electronic levels near the bands.

Manfredotti *et al.*[5] compared the properties of melt-grown and vapor-transport-grown GaTe crystals and found a higher hole concentration of $4.7\times10^{17}/\text{cm}^3$ in the former compared with $6.1\times10^{16}/\text{cm}^3$ in the latter. The principal acceptor levels were 74 and 152 meV above the valence band for the melt-grown and vapor-transport-grown GaTe, respectively. The main scattering mechanism was due to ionized impurities for $T<80$ K. Only in-plane properties were studied, the highest hole mobility being 50 $\text{cm}^2/\text{V s}$ in melt-grown and 50–100 $\text{cm}^2/\text{V s}$ in vapor-transport-grown crystals at 80 K. Impurity scattering was again identified as the principal scattering mechanism, the exponent of the $\log_{10}\mu$ vs $\log_{10}T$ curves being found to be 1.57, 1.48, and 1.70 for crystals grown by Bridgman, chemical transport, and sublimation techniques, respectively.

Brebner and Fischer[6] studied the fundamental absorption edge of cleaved GaTe crystals. At 300 K the peak occurred at 1.663 eV, and it split and shifted to 1.779 and 1.795 eV at 4.2 K. Study of the photoreflectance spectrum at 295 K showed a positive peak near 1.679 eV attributed to the $n=1$ exciton line. Wan *et al.*[7] presented photoluminescence and transmission measurements on vapor-grown GaTe. The ground state 1*s* triplet and singlet excitonic peaks were found be well resolved, the triplet state lying 1.6 meV lower than the singlet. However, to the best of the authors' knowledge, photoconductivity studies on GaTe single crystals have not been reported before.

A comprehensive study of the Bridgman growth, characterization, transport properties such as thermopower, resistivity, and Hall effect, and dielectric constants in single-crystal GaTe and InTe was taken up and some results have already been reported.[8,9] The hole concentrations in GaTe were found to be $(2.75-6.5)\times10^{15}/\text{cm}^3$ at 300 K. In-plane hole mobilities of 450–500 $\text{cm}^2/\text{V s}$ at 80 K were found, the highest reported in GaTe. Thermopower measurements along and perpendicular to layer planes yielded density-of-states hole effective masses of $m_{\parallel}^*=0.465m_0$ and $m_{\perp}^*=0.995m_0$ in

TABLE I. Conductivity anisotropy and activation energies in GaTe with doping between 80 and 250 K.

Sample	$\sigma_{\parallel}$ (Ω cm) 300 K	$\sigma_{\perp}$ (Ω cm) 300 K	$\sigma_{\parallel}, \sigma_{\perp}$ 80 K	$\sigma_{\parallel}, \sigma_{\perp}$ 300 K	E_a (meV) 80–100 K	E_a (meV) 100–250 K	E_a (meV) 80–100 K	E_a (meV) 100–250 K
Undoped	(3.33–4) $\times 10^{-2}$	(3.33–5) $\times 10^{-3}$	55–60	8–10	23	40	74	110
Ge doped	5.0×10^{-3}	2.46×10^{-4}	65	20	35	54	97	125
I_2 doped	1.67×10^{-3}	7.6×10^{-5}	68	22	42	62	154	221

good agreement with Schmid's scattering model. Deep-level studies[10] were also carried out, showing the presence of an acceptor level 0.45 eV above the valence band that traps holes at low temperatures. Thus electrons are considered to be the mobile carriers at $T<50$ K. The study of Schottky barriers on such an anisotropic semiconductor (GaTe) was reported,[11] the thermionic emission theory was verified, and the Richardson constants were shown to be in agreement with the experimentally determined hole effective masses.

In this paper we report a study of photoconductivity spectral response which showed a maximum at 747 nm (1.66 eV). The conduction mechanisms along and across the layer planes, which exhibit weak localization, hopping, and band conduction at temperatures between 10 and 80 K, have also been studied in detail. Negative magnetoresistance was observed for conduction both along and perpendicular to the layer planes at 10 K. The *I-V* characteristics showed evidence of quantized behavior due to carrier tunneling. The results of transport studies are interpreted as being influenced by stacking faults between the planes as observed by transmission electron microscopy (TEM).

II. GROWTH AND CHARACTERIZATION

The growth of GaTe single crystals has been carried out by various workers using the closed-tube sublimation technique,[12] iodine-assisted chemical transport,[13] and Bridgman-Stockbarger melt growth.[14,15] The last method was used in the present investigations. The phase diagram of the Ga-Te system shows a number of compounds such as GaTe having a melting point of 1097 K and Ga_2Te_3 with a melting point of 1063 K. GaTe was first synthesized by taking stoichiometric amounts of 99.9999% pure Ga and Te in high-purity silica tubes. Ga was etched in concentrated HCl and Te in $HCl:C_2H_5OH$ in the ratio 1:10 prior to loading. The quartz ampoules were evacuated to 10^{-6} torr before sealing. These were then slowly heated in a furnace to 1200 K, maintained at that temperature with constant rotation for melt homogenization for 12 h, and then slowly cooled at 50 °C/h. After synthesis the tip of the ampoule was connected to a thin 3-mm-diameter quartz rod for better nucleation during slow Bridgman growth. The ampoule was then placed in a vertical SiC furnace with good temperature control and connected to a slow-speed (0.1 rpm) motor. After heating to 1150 K and maintaining for 8 h, the ampoule was slowly lowered at a rate of 1.2 mm/h through a temperature gradient of 20 °C/cm to 400 °C. Finally the furnace was cooled to room temperature at 100 °C/h. The resulting hexagonal phase was metastable. A 30 min anneal at 110 °C caused conversion to the stable monoclinic phase. The ingots thus grown were 2–2.5 cm in length and 1.2 cm in diameter. Samples could easily be cleaved along the layer planes (parallel to the growth axis).

Impurity analysis of Ga, Te, and GaTe carried out using the inductively coupled plasma emission technique showed the principal impurities as Pb, Sn, Fe, and Mg at 0.67, 0.56, 0.34, and 0.26 ppm levels. Pb has been shown to give rise to *p*-type behavior in InSe, Sn gives *n*-type conduction, while Mg on the Ga site is expected to be a shallow acceptor. Thus the deep acceptor level observed in undoped GaTe, as discussed later, may be associated with Fe or with unspecified native defects. Energy-dispersive x-ray analysis (EDAX) and x-ray photoemission spectroscopy (XPS) studies were conducted to determine the crystal stoichiometry. The Ga content was found to be 49.2–49.3 % by EDAX and 49.1–49.2 % by XPS, the corresponding Te content being 50.8–50.7 % and 50.9–50.8 %, respectively.

The crystal structure of the grown crystal was determined by the powder diffraction technique. The spectra gave characteristic strong peaks for the (310), (003), (402), and (201) planes and yielded the following lattice parameters for the monoclinic structure: $a=17.32$, $b=4.05$, and $c=10.54$ Å with $\beta=104.4°$. The single-crystal nature was verified using the Laue back-reflection technique, which showed GaTe as having (001) orientation along the layer plane.

TEM and electron diffraction studies were performed on samples cleaved parallel to the basal plane. These were examined with a Philips 100 keV microscope. The diffraction patterns showed single-phase material with twofold symmetry characteristic of a monoclinic structure, the lattice parameters being consistent with those found by x-ray diffraction. The presence of extended lattice defects in the region examined gave rise to splitting of the higher-order spots. The TEM photographs showed the presence of partial dislocations in the basal plane. The dislocations divide the sample into ribbons of stacking faults as wide as 1 μm, which are separated from each other by unfaulted regions. Similar observations have been made of glide dislocations lying in the basal plane of GaSe.[16] The etch pit density, measured on the layer planes using $K_2Cr_2O_7$ diluted in H_2SO_4 as etchant, was found to be between 5×10^6 and $1\times 10^7/cm^2$.

Apart from nominally undoped *p*-type GaTe crystals, doping with 0.5% Ge and 0.5% I_2 as possible donors was also carried out with the aim of type conversion. This resulted in crystals with higher resistivity due to compensation, increased activation energies in both directions, and increase of

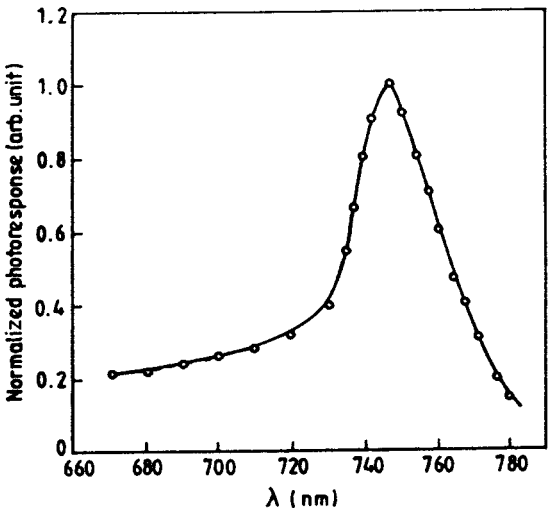

FIG. 1. Spectral response of photoconductivity in GaTe with conduction along layer planes and light incident perpendicularly.

the anisotropy factor as given in Table I. No type conversion was observed. With further increase in Ge concentration to form the alloy $Ga_{1-x}Ge_xTe$ ($x=0.15-0.50$), the dielectric constant increased and ferroelectric behavior was observed as already reported.[17] For *p*-type doping attempted with Zn, the anisotropy factor decreased, as also did the activation energies.

III. PHOTOCONDUCTIVITY

Optical absorption studies[9] on single crystals perpendicular to the layer planes gave a direct energy gap from linear $(\alpha h\nu)^2$ vs $h\nu$ plots of 1.66 ± 0.002 eV in good agreement with the reported value of 1.663 eV. Photoconductivity spectral response and gain studies were then conducted on samples typically $0.3\times0.3\times0.06$ cm^3. Evaporated In electrodes were used after annealing at 200 °C for 2 min. The sample was illuminated by a tungsten-halogen lamp through a grating monochromator with automatic aperture and intensity control in the spectral range of 600–800 nm. Samples were mounted in a liquid-nitrogen-cooled cryostat with quartz windows for low-temperature studies. Photocurrents were measured using a Keithley 160B digital multimeter capable of measuring down to 1 nA. The photoconductivity gain was studied using a 500 W tungsten lamp focused to give an intensity of 55 mW/cm^2 on the sample, as measured by a calibrated solar intensity meter.

The spectral response of photoconductivity (PC) in the layer plane normalized with respect to the peak at 747 nm (1.66 eV) is shown in Fig. 1. The measured response extends to 780 nm (1.589 eV) at longer wavelengths and saturates at a value of 0.22 at wavelengths shorter than 660 nm. The peak response is obtained at the optical band gap, the optical absorption actually extending to 1.40 eV. For wavelengths slightly longer than the band gap, the photon energy is insufficient to excite electron-hole pairs and hence absorption and photoresponse are low. For higher energies the absorption increases and the absorption depth decreases until at $h\nu \gg E_g$ the absorption occurs very near the surface where recombination may be high. It is known that the effective lifetime $\tau_{\rm eff}$ is determined by both bulk and surface lifetimes, τ_b and τ_s, respectively, i.e.,

$$1/\tau_{\rm eff}=1/\tau_b+1/\tau_s\,. \tag{1}$$

For a thin slab of thickness d it has been shown that $\tau_s=d/2s$, where s is the surface recombination velocity. Thus the location of the PC maximum depends on the relative importance of surface and bulk lifetimes as well as the sample thickness d compared with the absorption depth $1/\alpha$.

An exact expression for the spectral response of photoconductivity was derived by de Vore.[18] With some simplifying assumptions such as local electrical neutrality, steady and weak excitation, and absence of trapping, this can be written as

$$I_{\rm PC}=\frac{1-e^{-Z}}{1+R\coth(W/2)}\times\left\{1+\frac{RW[W\coth(W/2)-Z\coth(Z/2)]}{W^2-Z^2}\right\}, \tag{2}$$

where L is the diffusion length, l the specimen thickness, α the absorption coefficient, D the diffusion coefficient, τ the carrier lifetime, $W=1/L=1/(D\tau)^{1/2}$, $Z=\alpha 1$, and $R=s\tau/1$. De Vore has shown that a maximum in response occurs for $s\gg D/\tau$. Since α is not known for the entire wavelength region, the following three limiting cases can be taken: (i) $\alpha\ll 1/L$ at low energies, (ii) $\alpha\sim 1/L$ near the absorption edge, and (iii) $\alpha\gg 1/L$ at high energies. In the first case, the variation of $I_{\rm PC}$ with λ is determined by Z and effectively follows that of the absorption coefficient, $\alpha(\lambda)$. The second condition gives the response maximum. The last case can be used to determine s since in this region $Z\gg W$ and Eq. (2) can be simplified to

$$I_{\rm PC}=\frac{1+(RW/Z)}{1+R\coth(W/2)}\,. \tag{3}$$

In the present case the relative PC response saturates at a value of 0.22. This gives $R=29$ from Eq. (3) considering an arbitrarily large value of Z. From this s is found to be 4.3×10^4 cm/s. This is a reasonably low value, which can be compared with $s=10^3$ cm/s reported by Augelli *et al.*[19] for GaSe, which has a band gap of 2.0 eV.

The I-V characteristics of the samples both in the dark and with tungsten illumination (55 mW/cm^2) were studied in the different current flow directions and were found to be linear with applied voltage. The dark current I_d in the direction perpendicular to the layer plane was found to be smaller by a factor of ~6–8 at 300 K. The photoconductive gain defined as $(\Delta I/I_d)$, where $\Delta I=I_{\rm ph}-I_d$ ($I_{\rm ph}$ is the photocurrent), was determined for current directions both along and perpendicular to the layer plane and is plotted in Fig. 2. The higher value of $(\Delta I_\perp/I_d)$ compared with $(\Delta I_\parallel/I_d)$ is essentially due to the difference in dark current due to lower conductivity in this direction, as found earlier.[9] This is attributed to the existence of stacking faults between the layers, which create potential barriers. On illumination, the generated car-

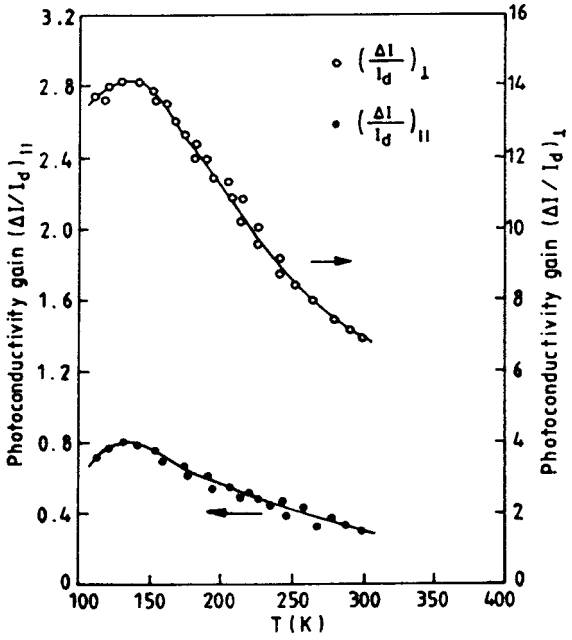

FIG. 2. Temperature variation of photoconductivity gain in GaTe with current flowing along layer planes (●) and perpendicular to layer planes (○).

riers neutralize the space charge due to the potential barriers and increase the effective hole mobility in this direction. The temperature dependence of the photoconductive gain shows maxima near 130 K in both directions while the hole mobilities show maxima at 80 K (see Fig. 10 below).

It is known that the photoconductive gain[20] depends on the light-induced conductivity $\Delta\sigma=\sigma_{\rm ph}-\sigma_d$, which is proportional to $I_{\rm ph}-I_d$ and is given by

$$\Delta\sigma=g_{\rm op}q(\mu_n\tau_n+\mu_p\tau_p) \tag{4}$$

where $g_{\rm op}$ is the rate of creation of electron-hole pairs per volume per s, μ_n,μ_p are the electron and hole mobilities, and τ_n,τ_p are the electron and hole lifetimes, respectively. Thus the temperature dependence will be determined by the variation of these parameters. The generation rate $g_{\rm op}$ can be calculated from the light intensity I,

$$g_{\rm op}=\alpha I/h\nu, \tag{5}$$

where α is the absorption coefficient and $h\nu$ the photon energy. Assuming that the photoconductivity is dominated by one carrier type, i.e., $\mu_p\tau_p\gg\mu_n\tau_n$, the carrier lifetime can be found from

$$\tau_p=\Delta\sigma/qg_{\rm op}\mu_p=\Delta\sigma h\nu/q\mu_p\alpha I. \tag{6}$$

The hole mobilities in the two directions and their variation with temperature were previously determined. These were found to be in the range 25–40 $\rm cm^2/V\,s$ in the layer plane and 10–15 $\rm cm^2/V\,s$ in the perpendicular direction at 300 K. The lifetimes were thus found to be $\tau_p=3.43\times10^{-7}$ s in the layer plane and 2.03×10^{-6} s in the perpendicular direction at 300 K.

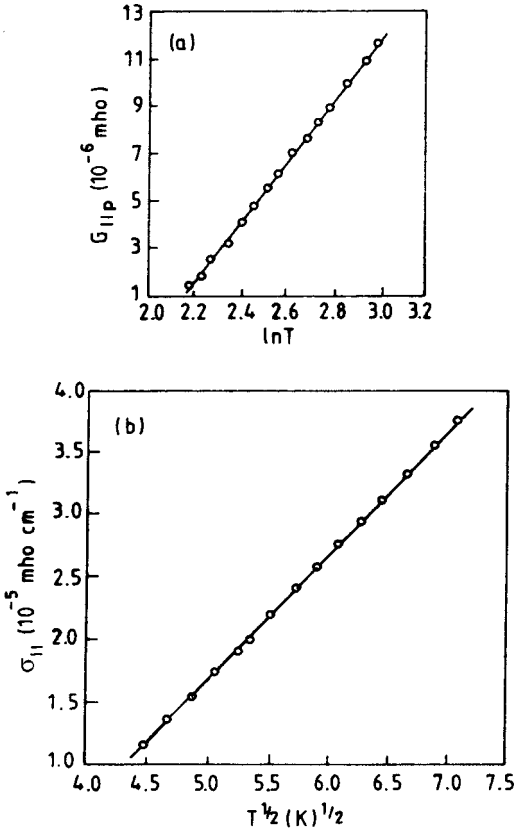

FIG. 3. (a) Temperature variation of conductance $G_{\parallel}$ along layer planes for $T=9-20$ K. (b) Temperature variation of conductivity $\sigma_{\parallel}$ along layer plane for $T=20-50$ K.

IV. LOW-TEMPERATURE CONDUCTIVITY STUDIES

Due to the anisotropy in electrical conduction observed at 300 K and the presence of natural barriers between planes in the direction normal to the layer planes, it was considered interesting to investigate conduction in orthogonal directions down to 10 K. Specimens were prepared from grown single-crystal ingots by cleavage, lapped and polished with alumina, and etched in $\rm HCl:HNO_3:10H_2O$. Samples were of final dimensions $4\times3\times0.08$ $\rm mm^3$. Contacts were prepared by alloying small In spheres on the sample plane for in-plane measurements and on two sides at the center of the specimens for measurements across the layer planes. Samples were placed in a closed-cycle He cryostat for conductivity measurements between 10 and 300 K. Magnetoresistance studies were carried out up to fields of 0.37 T.

Figure 3(a) shows the variation of conductance $G_{\parallel}$ in the layer plane between 9 and 20 K. There is very good fit with a linear variation of $G_{\parallel}$ with $\ln T$ according to the relation given by Lee and Ramakrishnan[21] valid for weak localization in two-dimensional conduction,

$$\Delta G=(\lambda e^2/\hbar)\ln T, \tag{7}$$

where $\lambda=\alpha p/2\pi^2$. From the slope of the experimental curve the value of λ is found to be 0.051 giving $p=1$ for a noninteracting electron gas for which $\alpha=1$. From the value of λ,

the value of $e^2/2\pi^2\hbar$ is found to be $1.23\times10^{-5}\,\Omega^{-1}$ which is in excellent agreement with the calculated value of $1.2306\times10^{-5}\,\Omega^{-1}$.

For temperatures between 20 and 50 K the in-plane conductivity $\sigma_\parallel$ is found to vary as $T^{1/2}$ as shown in Fig. 3(b). This is in accordance with weak localization in three dimensions with $p=1$, where

$$\sigma=(\beta e^2/2\pi^2\hbar D^{1/2})T^{p/2}, \tag{8}$$

where β like α is a product of constants. The slope of this linear plot is $1.25\times10^{-5}\,\Omega^{-1}\,\mathrm{cm}^{-1}$, which gives $D=1\ \mathrm{cm}^2/\mathrm{s}$ for $\beta=1$, not an unreasonable value. Shklovskii and Erfros[22] predicted a $T^{1/2}$ variation of conductivity at low temperatures due to variable-range hopping in the presence of long-range Coulomb interactions, which is an alternative model to weak localization.

Perpendicular to the layer planes the variation of conductance with temperature is quite different, primarily due to the existence of stacking faults which create potential barriers of several tens of meV. In the Mott[23] theory of hopping conduction at low temperatures due to carriers moving in a narrow band near the Fermi level, the temperature dependence of conductance for a three-dimensional system is given by

$$G(T)=G_0\exp(T/T_0)^{1/4} \tag{9a}$$

with

$$T_0=\beta/kg(\mu)a^3, \tag{9b}$$

where $g(\mu)$ is the density of states near the Fermi level, a is the localization radius of states near the Fermi level, and β is a numerical coefficient. In a system with localized states near the Fermi level in which the density of states can be regarded as constant, $g(E)=g(\mu)$ provided $g(\mu)\#0$ at sufficiently low temperature.

In the case of motion restricted to two dimensions, $g'(\mu)$ is the two-dimensional density of states at the Fermi level, and Mott's law becomes

$$G(T)=G_0\exp(T/T_0^*)^{1/3} \tag{10a}$$

with

$$T_0^*=\beta^1/kg''(\mu)a^2. \tag{10b}$$

Between 9 and 20 K the linear variation of $\ln G_\perp$ vs $T^{1/3}$ shown in Fig. 4(a) is characteristic of hopping in two dimensions. The slope gives $T_0^*=0.057$. At slightly higher temperatures 20–50 K $\ln G_\perp$ is found to be proportional to $T^{1/4}$ as in Fig. 4(b) with $T_0=0.0256$ found from the slope of the plot. It is found that a crossover occurs with increasing temperature, from a $(T_0/T)^{1/3}$ to a $(T_0/T)^{1/4}$ variation, which is characteristic of Mott hopping in three dimensions. The variations of conductivity at low temperatures in two different directions which are unusual for a single material are summarized in Table II.

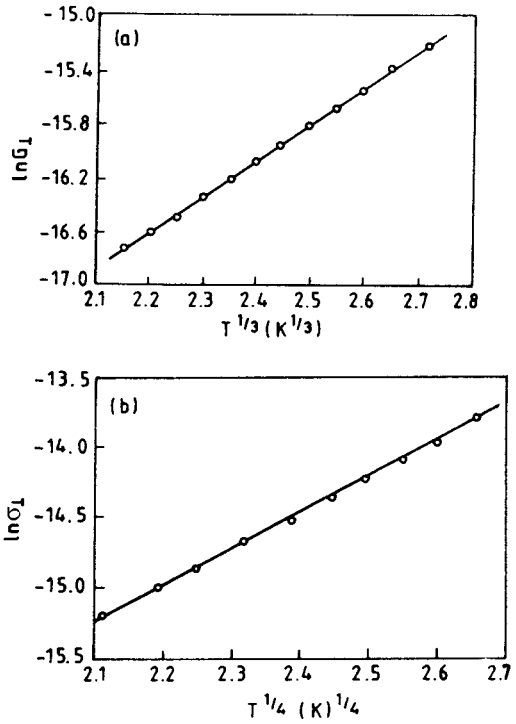

FIG. 4. (a) Temperature variation of conductance $G_\perp$ perpendicular to layer planes for $T=9-20$ K. (b) Temperature variation of conductivity $\sigma_\perp$ perpendicular to layer planes for $T=20-50$ K.

V. MAGNETORESISTANCE

The two-dimensional character of conduction parallel to the layer plane was manifest in the form of negative magnetoresistance observed in the temperature range 9–20 K. The transverse magnetoconductance measured in the layer plane at 10 K is shown in Fig. 5(a) as a function of both directions of H at low fields. This is due to suppression of weak localization as first observed by Eisele and Dorda[24] in high-quality Si metal-oxide-semiconductor field-effect transistors (MOSFET's) and also by other groups in agreement with the theoretical formulation of Hikami *et al.*[25] and Al'tshuler *et al.*[26] Negative magnetoresistance with a quadratic field dependence at small fields has been observed experimentally in a number of insulating materials in the hopping regime, including n-Ge, In_2O_3, n-GaAs, and n-CdSe.[27]

The increase of magnetoconductance has an H^2 dependence as show in Fig. 5(b), as predicted by Eq. (9) in the weak-field limit. Along the direction normal to the layer planes similar behavior was also observed as shown in Fig. 6. An H^2 variation was again found, given by the relation

TABLE II. Nature of variation of conductivity for conduction along and perpendicular to layers between 10 and 50 K.

	T	
Crystal direction	9–20 K	20–50 K
Parallel to layer plane	$G_\parallel\propto\ln T$	$\sigma_\parallel\propto T^{1/2}$
Perpendicular to layer plane	$G_\perp\propto\exp(T/T_0)^{1/3}$	$\sigma_\perp\propto\exp(T/T_0)^{1/4}$

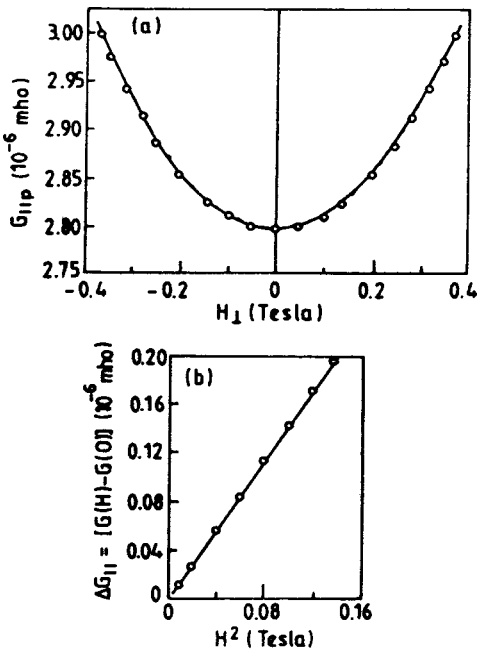

FIG. 5. (a) Variation of magnetoconductance in layer plane, $G_\parallel$, with H at 10 K. (b) Variation of $\Delta G_\parallel$ with H^2 at 10 K.

$$\Delta R_\perp / R_\perp = f(T) H^2 = R_{\rm hop}^3 H^2. \tag{11}$$

The slopes of the curves plotted as a function of H^2 in Fig. 6 yield the function $f(T)$ and are expected to reflect the temperature dependence of $R_{\rm hop}$, i.e., $f(T) \sim R_{\rm hop}^3 \sim T^{-1}$ as observed from the plot in Fig. 7 where $R_{\rm hop} \sim T^{-1/3}$. With increasing temperature the negative magnetoresistance decreases as shown in Fig. 6 but does not change sign or disappear at $T = 20$ K.

Negative longitudinal magnetoresistance was also observed at 10 K with conduction in the layer plane. This also occurs due to suppression of the weak-localization correction as observed by Mensz and Wheeler[28] in Si inversion layers and by Lin *et al.*[29] in GaAs/Al_xGa_{1-x}As heterostructures.

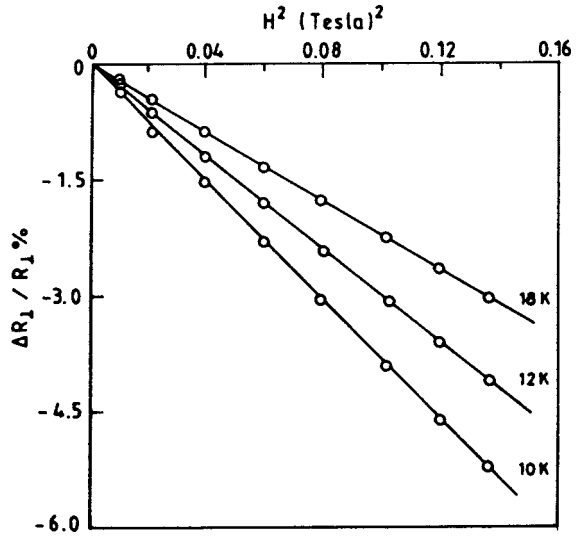

FIG. 6. Variation of $\Delta R_\perp / R_\perp$ with H^2 at 10, 12, and 18 K.

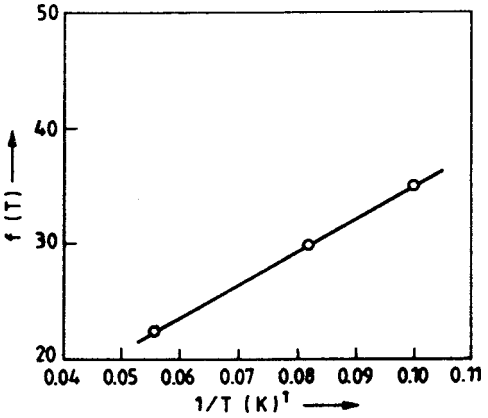

FIG. 7. Variation of the function $f(T)$ with $1/T$.

For negative magnetoresistance as observed by Eisele and Dorda[24] in high-quality Si MOSFET's, H_c was estimated to be ~0.0030 T due to the high electron mobility. For MOSFET's with lower mobility H_c was found to be as high as a few kilogauss. In the case of GaTe with low electron mobility, H_c is found to be ~0.05 T.

Above 80 K positive transverse magnetoresistance was observed in both current flow directions with an H^2 variation as shown in Fig. 8. This is due to the expected decrease in the hole mean free path in three dimensions with magnetic field, the variation being given by

$$\Delta\rho/\rho = \text{const} \times (eHL/mcv)^2 = kH^2. \tag{12}$$

The results of magnetoresistance measurements are summarized in Table III.

VI. *I-V* CHARACTERISTICS

The *I-V* characteristics were studied with the same electrode configurations as before both in and across the layer planes at 10 K with electric fields between 0.05 and 0.85 V/cm. While the current was higher by an order of magnitude and increased smoothly with the applied voltage in the layer plane, across the plane the characteristics were found to exhibit discrete steps (Fig. 9) up to fields of 0.55 V/cm which

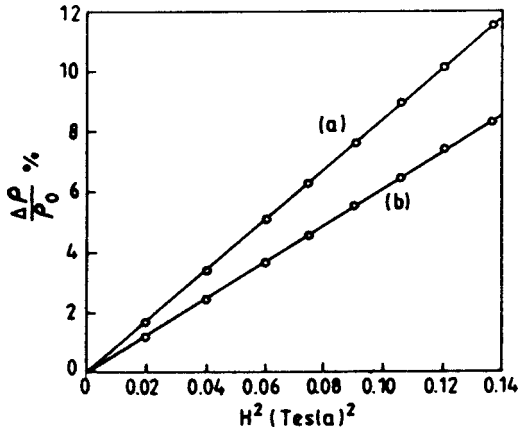

FIG. 8. Variation of positive magnetoresistance $\Delta\rho/\rho$ (a) in the layer plane and (b) perpendicular to the layer plane at 80 K.

TABLE III. Variation of magnetoresistance (%) along and perpendicular to layer planes at 10 and 80 K.

Crystal direction	$\Delta\rho/\rho$ $T=10$ K	$T=80$ K
Parallel to layer plane	−7.14	+11.5
Perpendicular to layer plane	−5.18	+8.3

disappeared when the temperature increased to 25 K. This may be attributed to the existence of quasibound states created by the presence of stacking faults between the layers.

Although at room temperature GaTe shows *p*-type conductivity, it was shown through deep-level transient spectroscopy studies[10] that deep acceptor levels exist which trap holes at low temperatures and hence the mobile carriers at 10–50 K are considered to be electrons.

The application of an electric field causes carrier tunneling between the confined states when they are brought into alignment by an electric field while further bias destroys this alignment. It is assumed that the applied voltage is nonuniformly distributed, most of it appearing across a few barriers created by stacking faults. At still higher fields and at higher temperatures the carriers are excited above the barriers and the current increases monotonically. The presence of stacking faults can thus be considered to create a natural superlattice.

VII. DISCUSSION

As a consequence of the disorder present in these layered III-VI compounds, the possibility of observation of Anderson localization at sufficiently low temperatures is present when electrons are confined to move along the layer planes. This has indeed been observed in InSe by El-Khatouri *et al.*,[30] who studied the temperature variation of conductance in one direction only. It was also shown by Maske and Schmid[31] that in layered crystals such as GaSe and InSe disorder due to stacking faults is sufficient to localize electron states along the layer normal, carrier transport taking place via hopping conduction in this direction.

It is interesting to note that the variation of mobility with

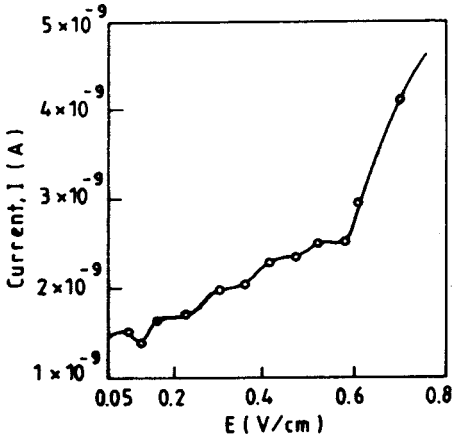

FIG. 9. *I-V* characteristic across layer plane at $T=10$ K.

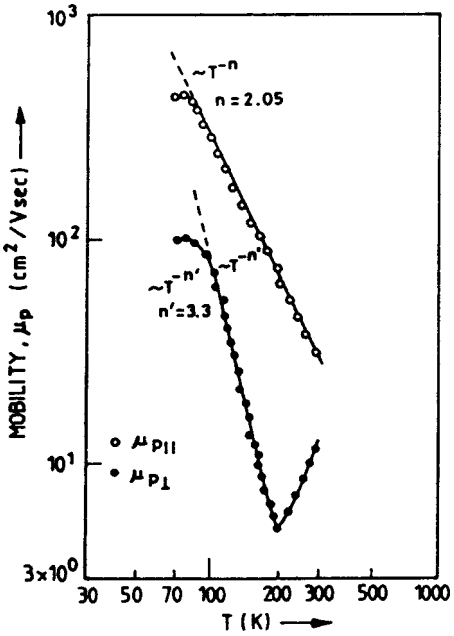

FIG. 10. Variation of hole mobility with temperature between 80 and 300 K along and perpendicular to the layer planes.

temperature perpendicular to the layer planes (Fig. 10) in the present samples near 200 K also reflected the presence of stacking faults with possible impurity segregation. Thus, while $\mu_\perp$ decreased in the range 100–200 K due to homopolar optical phonon scattering, it showed an anomalous increase with temperature above 200 K with an activation energy of 40 meV. Similar behavior was also reported for InTe by Hussain[32] and also attributed to the presence of stacking faults. The variation in mobility along the layer plane, on the other hand, did not show any such anomaly.

Conduction in the layer plane showed $\ln T$ behavior between 9 and 20 K and $T^{1/2}$ variation between 20 and 50 K with the slopes giving accurate values of the constants given by Eqs. (7) and (8). In the perpendicular direction, the Mott laws for hopping conduction in two and three dimensions were found to be obeyed.

Negative magnetoresistance was observed for conduction in both directions below 50 K irrespective of the exact conduction mechanism. Although the magnitude decreased with increase in temperature, it did not disappear at the crossover from the Mott law regime to the $T^{1/2}$ law regime near 20 K.

VIII. CONCLUSIONS

The spectral response of photoconductivity showed a maximum at 1.66 eV at the optical band gap of GaTe. From the short-wavelength response the surface recombination velocity was estimated. Photoconductive gain measurements enabled the determination of majority-carrier lifetimes along and perpendicular to the layer planes.

Weak localization in two dimensions was found in GaTe for conduction in the layer plane between 10 and 20 K with conductance increasing as $\ln T$. The slope of the plot gave the exact value of $e^2/2\pi^2\hbar$. This localization is attributed to the confinement of the carriers in two dimensions by natural

stacking faults. Negative magnetoresistance was observed in this temperature range due to suppression of weak localization by the applied magnetic field. Between 20 and 50 K hopping conduction with variation of conductivity as $T^{1/2}$ was observed due to weak localization in three dimensions, the slope giving the value of the diffusion coefficient D. In the direction perpendicular to the layer plane at 10–20 K, hopping conduction in two dimensions through or between the stacking faults was observed with $G_{\perp} \sim \exp(T/T_0)^{1/3}$, with a crossover to three-dimensional hopping conduction above 20 K with variation $\sim \exp(T/T_0)^{1/4}$. Negative magnetoresistance was also found in these cases while above 80 K positive magnetoresistance was observed for both current flow directions. I-V characteristics indicated tunneling transport across the layer planes due to potential barriers attributed to natural stacking faults.

ACKNOWLEDGMENTS

S.P. would like to thank the University Grants Commission, New Delhi for the financial support under which this work was carried out. The authors are grateful to A. R. Haldar for excellent technical assistance.

[1] R. C. Fivaz and P. E. Schmid (unpublished).
[2] A. Koma and J. Yoshimura, Surf. Sci. **174**, 556 (1986).
[3] N. Teraguchi, F. Kato, M. Konagai, and K. Takahashi, J. Electron. Mater. **20**, 247 (1991).
[4] G. Fischer and J. L. Brebner, J. Phys. Chem. Solids **23**, 1363 (1962).
[5] C. Manfredotti, R. Murri, A. Rizzo, L. Vasanelli, and G. Mirocci, Phys. Status Solidi B **65**, 249 (1975).
[6] J. L. Brebner and G. Fischer, in *Proceedings of the International Conference on the Physics of Semiconductors, Exeter*, edited by A. C. Strickland (IOP, London, 1962), p. 760.
[7] J. Z. Wan, J. L. Brebner, R. Leonelli, and J. T. Graham, Phys. Rev. B **46**, 1468 (1992).
[8] S. Pal, D. N. Bose, S. Asokan, and E. S. R. Gopal, Solid State Commun. **80**, 9753 (1991).
[9] S. Pal and D. N. Bose, Solid State Commun. **80**, 9 (1996).
[10] D. Pal, S. Pal, and D. N. Bose, Bull. Mater. Sci. **17**, 347 (1994).
[11] D. N. Bose and S. Pal, Philos. Mag. B **75**, 311 (1997).
[12] A. M. Mancina, C. Manfredotti, A. Rizzo, and G. Micocci, J. Cryst. Growth **21**, 187 (1974).
[13] V. L. Cardetta, A. M. Mancini, C. Manfredotti, and A. Rizzo, J. Cryst. Growth **16**, 155 (1972).
[14] Th. Karakostas, J. G. Antonopoulos, S. Kokkou, G. L. Bleris, and N. A. Economou, Phys. Status Solidi A **59**, K17 (1980).
[15] V. L. Cardetta, A. M. Mancini, and A. Rizzo, J. Cryst. Growth **16**, 183 (1972).
[16] Z. S. Basinski, D. B. Dove, and E. Mooser, J. Appl. Phys. **34**, 469 (1963).
[17] D. N. Bose and S. Pal, Mater. Res. Bull. **29**, 2111 (1994).
[18] H. B. de Vore, Phys. Rev. **102**, 86 (1956).
[19] V. Augelli, C. Manfredotti, R. Murri, R. Piccolo, and L. Vasanelli, Phys. Rev. B **18**, 5484 (1978).
[20] R. H. Bube, *Photoconductivity of Solids* (Wiley, New York, 1960).
[21] P. A. Lee and T. V. Ramakrishnan, Rev. Mod. Phys. **57**, 287 (1985).
[22] B. I. Shklovskii and A. L. Efros, *Electronic Properties of Doped Semiconductors*, Vol. 45 of *Springer Series in Solid-State Sciences* (Springer, Berlin, 1984).
[23] N. F. Mott, J. Non-Cryst. Solids **1**, 1 (1968).
[24] I. Eisele and G. Dorda, Phys. Rev. Lett. **32**, 1366 (1974).
[25] S. Hikami, A. L. Larkin, and Y. Nagaoka, Prog. Theor. Phys. **63**, 707 (1980).
[26] B. L. Al'tshuler, A. G. Aonov, A. I. Larkin, and D. E. Khmel'nitskii, Sov. Phys. JETP **54**, 411 (1981).
[27] Y. Zhang and M. P. Sarachik, Phys. Rev. B **43**, 7212 (1991).
[28] P. M. Mensz and R. G. Wheeler, Phys. Rev. B **35**, 2844 (1987).
[29] B. J. Lin, M. A. Paalnen, A. C. Gossard, and D. C. Tsui, Phys. Rev. B **29**, 927 (1984).
[30] D. El-Khatouri, A. Khater, M. Balkanski, M. Julien, and J. P. Guesdon, J. Appl. Phys. **66**, 2049 (1989).
[31] K. Maschke and Ph. E. Schmid, Phys. Rev. B **12**, 4312 (1975).
[32] S. A. Hussain, Cryst. Res. Technol. **24**, 635 (1989).